Modified PIFA Array Design with Improved Bandwidth and Isolation for 5G Mobile Handsets

Naser Ojaroudi Parchin[*1], Yasir I. A. Al-Yasir[1], Haleh Jahanbakhsh Basherlou[2], Ahmed M. Abdulkhaleq[1, 3], Maryam Sajedin[4, 5], Raed A. Abd-Alhameed[1], and James M. Noras[1]

[1] Faculty of Engineering and Informatics, University of Bradford, Bradford BD7 1DP, UK
[2] Bradford College, Bradford, West Yorkshire, BD7 1AY, UK
[3] SARAS Technology Limited, Leeds LS12 4NQ, UK
[4] Instituto de Telecomunicações, Aveiro, Portugal
[5] Universidade de Aveiro, Aveiro, Portugal
[*]N.OjaroudiParchin@Bradford.ac.uk

***Abstract* —A new design of MIMO antenna array for fifth generation (5G) mobile handsets is proposed in this manuscript. The configuration of the design consists of eight planar-inverted F antenna (PIFA) elements located at different corners of the smartphone printed circuit board (PCB). The employed substrate is a low-cost FR-4 laminate with an overall size of 75×150×0.8 mm^3. For ease integration and design facilitation, the antenna elements and ground plane are etched on the same layer. By adding an arrow-shaped branch-strip between two adjacent PIFA elements, the impedance bandwidth and isolation characteristics are improved significantly. However, the whole antenna structure remains very simple and compact. The designed MIMO antenna provides good efficiencies and sufficient gains at the desired frequency band. Wide impedance bandwidth ($S_{11} \leq$ -10 dB) of 3.25-3.85 GHz has been obtained for each radiator. In addition, the isolation among antenna elements is less than -15 dB at the center frequency. The calculated TARC and ECC of the antenna elements are very low over the whole band of interest. Furthermore, the proposed design exhibits sufficient performance in the presence of user-hand.**

***Keywords* —5G, bandwidth improvement, decoupling, PIFA.**

I. Introduction

MIMO technology is a key component and probably the most promising technology to reach the transfer data rates of 5G cellular communications [1-2]. It can enhance channel capacity and link reliability of wireless systems [3]. A MIMO mobile-phone system needs a number of antenna elements which operate concurrently to achieve system diversity gain [4]. Recently, several MIMO antenna designs have been introduced for 5G cellular systems [5-12]. However, these mobile-phone antenna designs either exhibit narrow impedance-bandwidth or occupy a huge space or use non-planar elements.

Placing multiple antennas in the limited space of mobile-phone PCB poses a significant challenge in the incorporation of the MIMO technique. The closely-spaced antenna elements not only have to be impedance matched but also effectively isolated/decoupled from the neighboring MIMO antennas [13]. As far as decoupling is concerned, one of the methods is to place antennas far apart. However, this method is not efficient as it is wasteful of space. Therefore, an efficiently designed decoupling/isolation structure isolates all the antenna elements while not compromising space [14-15]. We propose here a new method to improve the bandwidth and isolation characteristics of the adjacent PIFA elements for 5G mobile handsets.

The PIFA is a popular and relatively low-profile antenna characterized by an omnidirectional radiation pattern [16-17]. Single-resonant, low-profile configurations of PIFAs suffer from an impedance-bandwidth limitation [18]. The proposed MIMO PIFA system is designed to operate at 3.5 GHz, a candidate frequency band for sub-6-GHz 5G cellular networks, proposed by Ofcom, UK [19]. To achieve enhanced isolation/decoupling among the adjacent elements, an arrow-shaped decoupling strip is employed. The design exhibits impedance match as well as isolation over the frequency band of 3.2-3.9 GHz. Fundamental properties of the MIMO design in terms of S parameters, efficiency, radiation pattern, ECC, TARC are investigated. The CST software was used to investigate the antenna characteristics [20].

II. Convectional PIFA Array

The design procedure for the proposed MIMO antenna is simple and straight forward. The first step is to start with a simple conventional PIFA, which is basically a short-circuited quarter-wave strip that provides single-resonance with the narrow bandwidth. Figure 1 illustrates the structure of the MIMO smartphone antenna with eight PIFA elements. The antenna elements are compact and located at corners of the PCB.

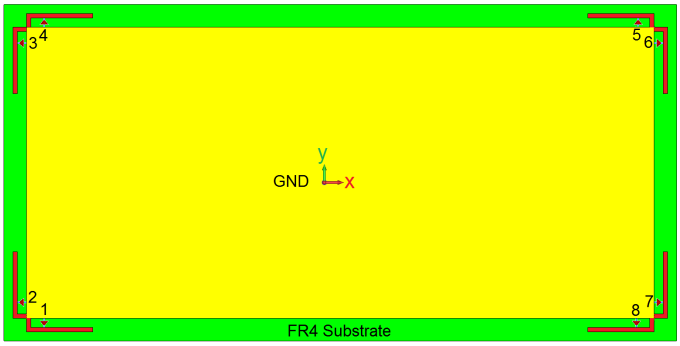

Fig. 1. Configuration of the conventional PIFA array.

Figure 2 illustrates the simulated S parameters (including S_{nn} and S_{mn}) of the conventional PIFA design. As can be observed from Fig. 2 (a), the antenna elements provide 200 MHz (3.4-3.6 GHz) bandwidth for $S_{11} \leq$ -10 dB with a single resonance at 3.5 GHz. In addition, the mutual coupling among the antenna elements is around -8 dB, as illustrated in Fig. 2 (b).

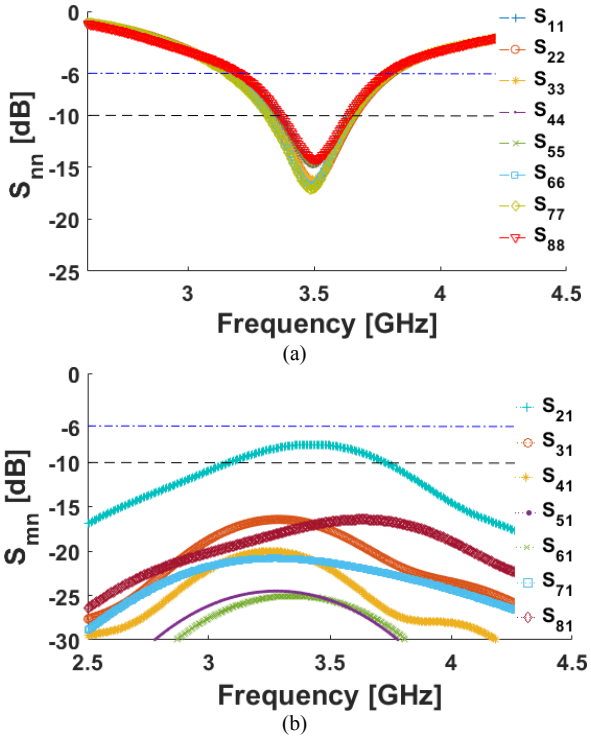

Fig. 2. (a) S_{nn} and (b) S_{mn} results of the conventional PIFA array design.

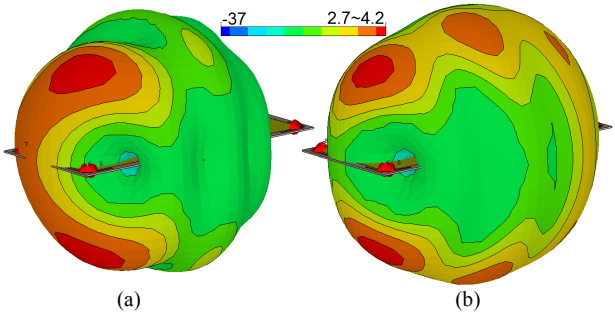

Fig. 3. 3D radiation patterns of (a) Ant.1 and (b) Ant. 2.

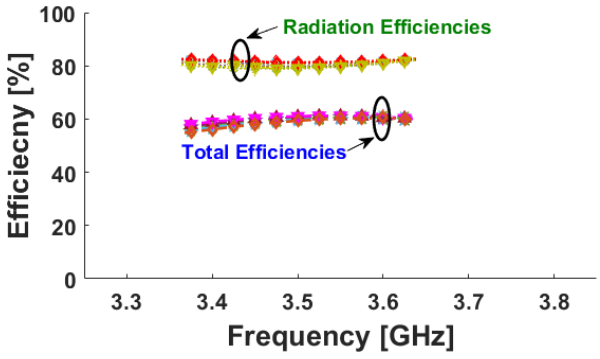

Fig. 4. Efficiencies of the PIFA array.

Figure 3 depicts 3D radiation patterns of two adjacent PIFA elements at the resonance frequency. As seen, the antenna elements have quasi-omnidirectional radiation patterns covering the top and bottom portions of the mobile-phone PCB. In addition, as can be observed from Fig. 4, the MIMO antenna provides sufficient efficiencies: more than 60% radiation and total efficiencies are achieved over the entire operation band.

III. The Proposed Modified PIFA Array Design

The configuration of the proposed design with modified PIFA radiators is shown in Fig. 5. It contains eight radiators printed on the FR-4 substrate with a dimension of 75×150 mm^2. Its parameters (in mm) are as follow: W=1, W_1=5, W_2=2, W_3=14.75, L=1, L_1=16, and x=1. As seen, the radiating elements and ground plane are etched on the same layer of the substrate to ease of integration with the circuits system. As illustrated, an arrow-shaped branch-strip has been protruded between two adjacent PIFA elements, which can improve the performance of each antenna element [21-22].

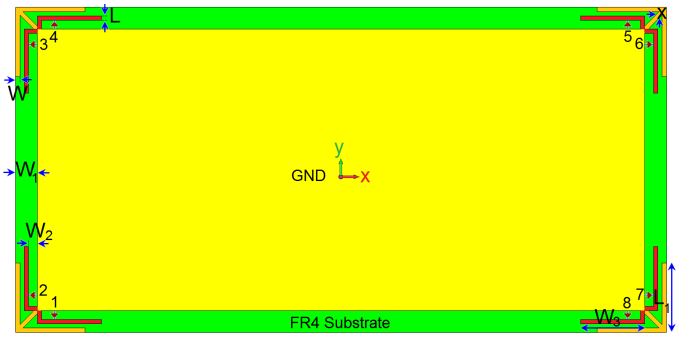

Fig. 5. Schematic of the proposed MIMO design.

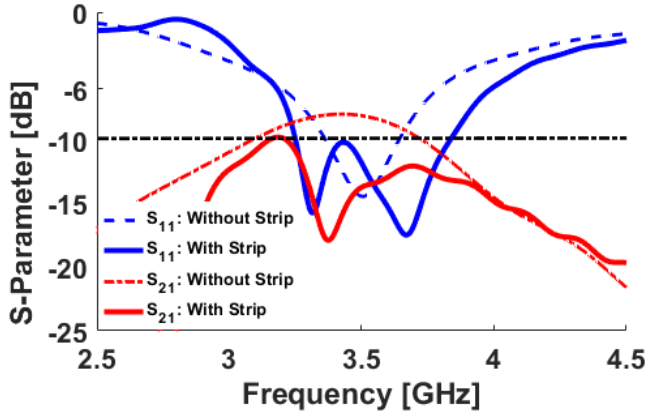

Fig. 6. S-parameters of two PIFA elements with/without the arrow-shaped strip.

Figure 6 shows the comparison of S-parameters for two PIFAs with and without the employed arrow-shaped strip. As can be observed, the conventional PIFA element resonates at 3.5 GHz providing 200 MHz for -10 dB impedance matching. In addition, its mutual coupling function is -8 dB. However, by adding the arrow-shaped branch-strip between, the impedance bandwidth and isolation characteristics have been improved significantly [23]. It is evident that more than 600 MHz bandwidth with low mutual-coupling (less than -15 dB) are achieved for the modified design.

In order to better understand the phenomenon behind this improved performance of the modified PIFA, the simulated current distribution of a single-element at 3.3 and 3.7 GHz (resonance frequencies) are studied in Fig. 7. As shown in Fig. 7 (a), the employed arrow-shaped strip is highly active at 3.3 GHz which verify its impact in creating the dual-resonance characteristic of the modified design [24-25]. It is observed that the second resonance of the design is occurred by the main radiators.

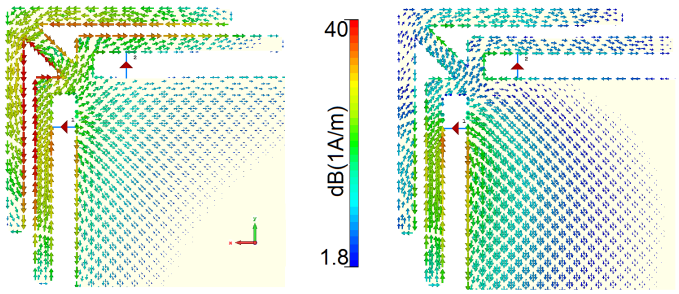

Fig. 7. Current distributions at (a) 3.3 and (b) 3.7 GHz.

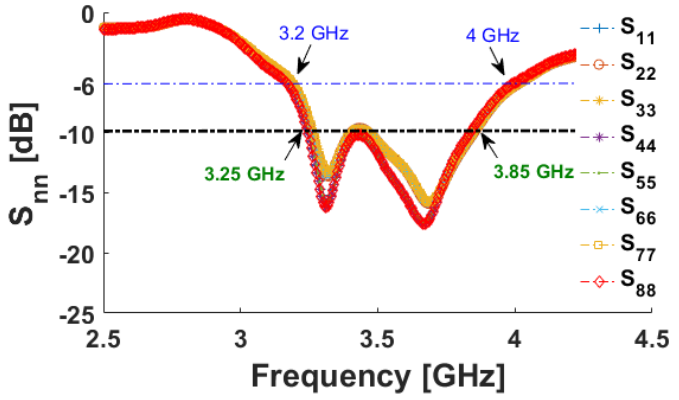

Fig. 8. (a) S_{nn} and (b) S_{mn} results of the modified PIFA array design.

Figures 8 (a) and (b) illustrate the simulated S_{nn} (refection confident) and S_{mn} (mutual-coupling) characteristics of the proposed 5G mobile-handset antenna, respectively. The design exhibits good S parameters with a broad bandwidth of 500 MHz (3.3-3.9 GHz) and reduced isolations of better than -15 dB. 3D radiation patterns of the proposed mobile-phone antenna design at 3.5 GHz are displayed in Fig. 9. It can be seen that each side of the mobile-phone PCB has been covered with differently polarized radiation patterns, due to orthogonally placement of the radiators. In addition, the gain levels of the elements vary from 2.8 to 4 dB. Thus, the MIMO antenna exhibited good radiation coverage with sufficient gain levels for each radiator.

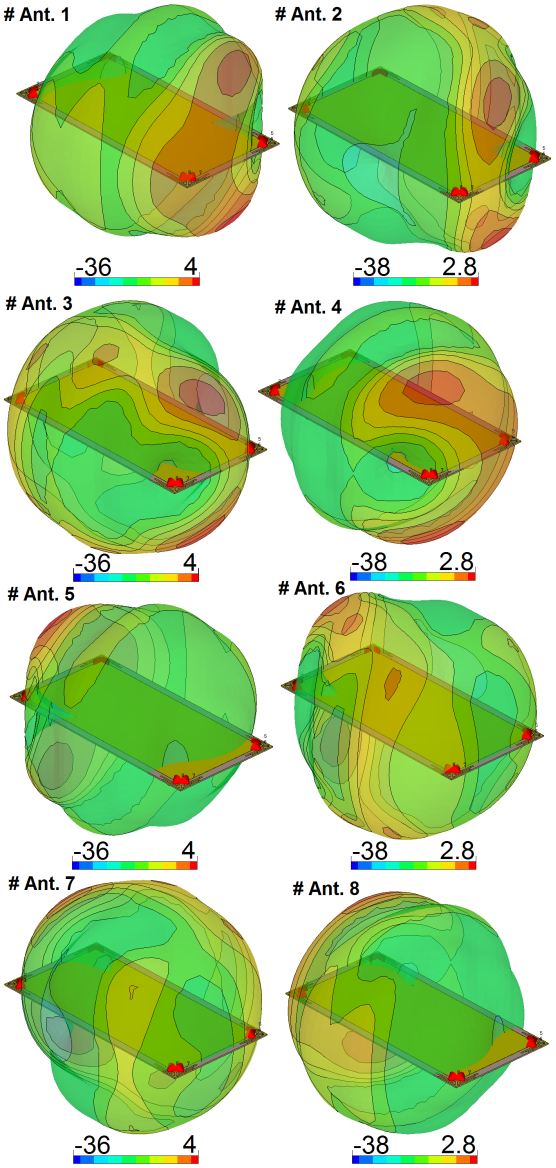

Fig. 9. 3D radiation patterns of the antenna elements at 3.5 GHz.

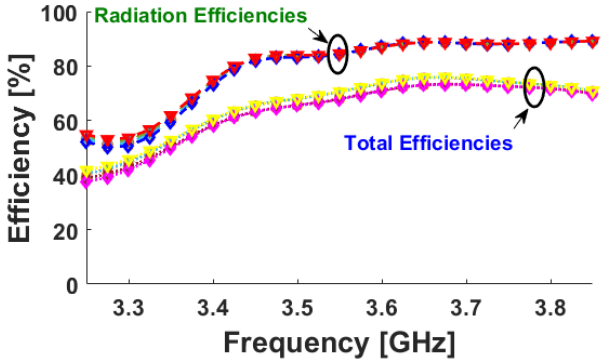

Fig. 10. Efficiency results of the MIMO design.

Furthermore, the designed MIMO antenna provides good radiation and total efficiencies over the operation band, as illustrated in Fig. 10: more than 80% radiation efficiency and 60% total efficiency properties are obtained for the radiation elements at the frequency range of 3.4-3.8 GHz (required 5G band).

Total active reflection coefficient (TARC) and envelope correlation coefficient (ECC) characteristics are two important parameters to be considered in MIMO antennas [26-27]. For MIMO systems, traditional scattering matrixes are not sufficient to predict the real antenna performance. ECC function signifies how the two closely-spaced antennas are coupled to each other, TARC which take coupling effect into account has been introduced. The ECC and TARC of two elements can be calculated from the S-parameters using the formula described as:

$$ECC = \frac{|S_{mm}^{*}S_{nm}+S_{mn}^{*}S_{nn}|^2}{(1-|S_{mm}|^2-|S_{mn}|^2)(1-|S_{nm}|^2-|S_{nn}|^2)^{*}} \quad (1)$$

$$TARC = -\sqrt{\frac{(S_{mm}+S_{mn})^2+(S_{nm}+S_{nn})^2}{2}} \quad (2)$$

The ECC and TARC characteristics of the mobile-phone antenna are represented in Fig. 11. As evident from figures, the calculated ECC results are very low entire the operation bands (less than 0.005). It can be also observed that the TARC value of the design is less than -30 dB at 3.5 GHz.

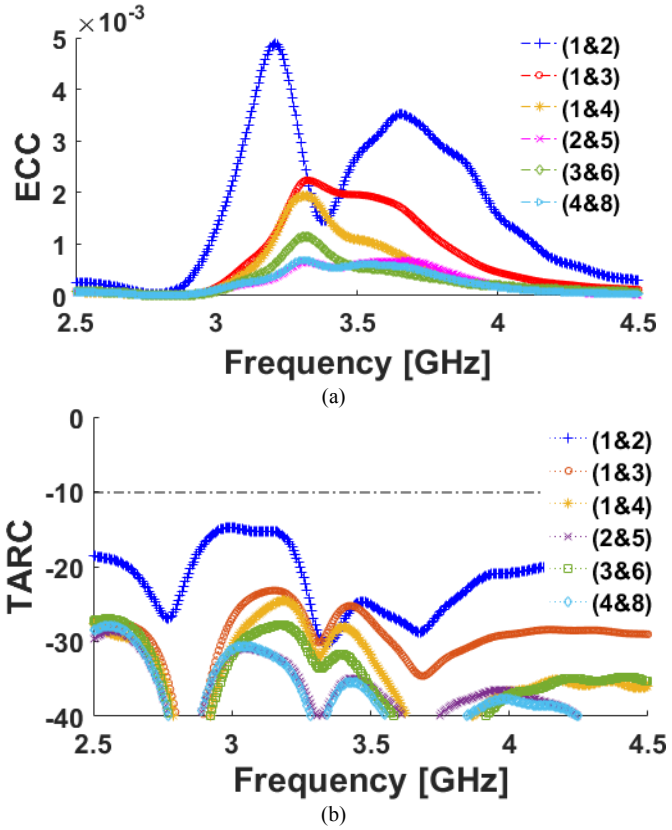

Fig. 11. (a) ECC and (b) TARC results of the proposed design.

The proposed modified PIFA array is fabricated for measurements. It is constructed on a cheap FR4 dielectric with an overall dimension of 75×150×1.6 mm^3 shown in Fig. 12 (a). Figure 12 (b) illustrates the feeding mechanism of the adjacent PIFA elements. As seen, a coaxial cable was used for feeding each antenna. It should be noted that the inner conductor of the coaxial cable was extended from the ground plane to the PIFA arm. Figure 13 comprises the measured and simulated S-parameters of the elements: the fabricated antenna operates properly with an acceptable agreement with the simulations.

Fig. 12. (a) Fabricated prototype and (b) feeding mechanism of two elements.

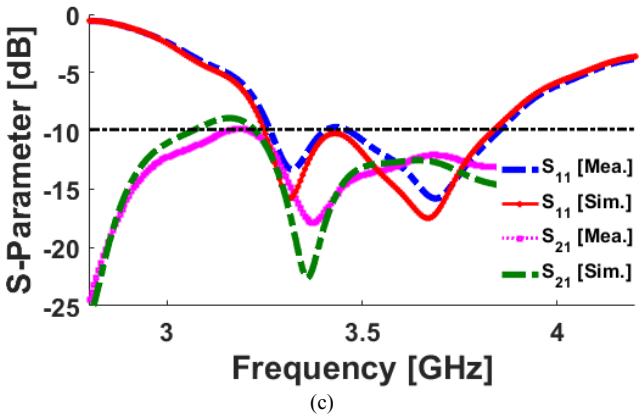

Fig. 13. Measured and simulated S-parameters of the two modified PIFAs.

IV. SAR and User-Hand Effect

Specific absorption rate (SAR) is a critical issue for mobile systems which is defined as the measurement function for the electromagnetic absorption of a user body during radio frequency transmissions [28].

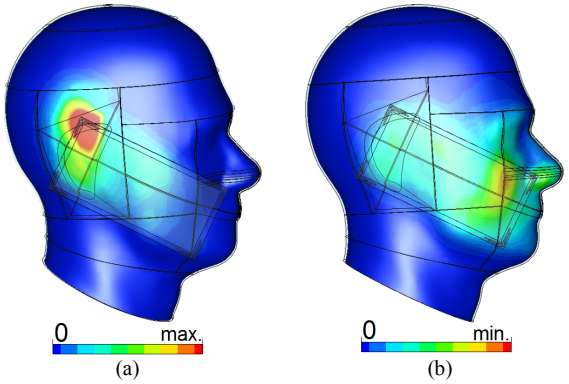

Fig. 14. SAR function of (a) Ant. 4 and (b) Ant. 7.

The SAR function of the design with user-head is investigated. As can be observed from Fig. 14, the maximum SAR value of the design is from Ant. 3 and the minimum SAR is absorbed from Ant. 7. According to the obtained results, it can be concluded that the distance between the antenna and the human-head has a significant impact on the SAR values. Different scenarios of the user-hand including right-hand and left-hand modes for top-layer/back-layer are studied in Fig. 15. Due to the symmetric configuration of the design, the MIMO antenna performs almost similarly for different hand scenarios. As can be observed the MIMO design and its radiation elements provide sufficient efficiencies (25%-65%). The maximum reductions of the antenna efficiencies are observed for the antenna elements partially covered by the user's hand.

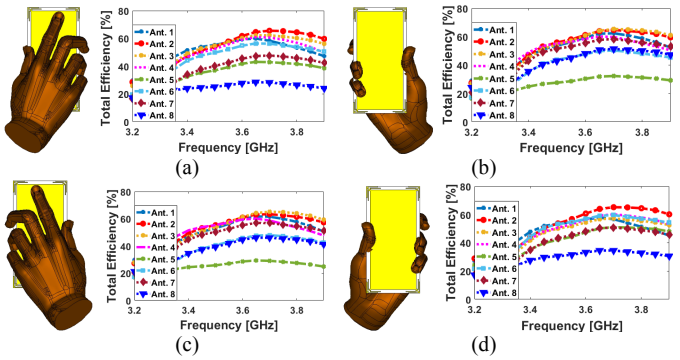

Fig. 15. Placement and Efficiencies of the design for different scenarios, (a) right-hand/top-layer, (b) right-hand/back-layer, (c) left-hand/top-layer, and (d) left-hand/back-layer.

V. Conclusion

Mobile-phone antenna design with modified PIFA elements is introduced for 5G mobile handsets. By adding an arrow-shaped branch-strip between each pair of closely-spaced PIFA elements, the impedance-bandwidth and isolation characteristics have been improved. S parameters, radiation patterns, efficiency, ECC, and TARC results of the design are studied and sufficient results are achieved. In addition, a prototype of the mobile-phone antenna was fabricated and S-parameters of two adjacent elements were measured. Moreover, SAR and different user-hand scenarios are investigated.

Acknowledgment

This work is supported by the European Union's Horizon 2020 research and innovation programme under grant agreement H2020-MSCA-ITN-2016 SECRET-722424.

References

[1] J. Rodriguez, *et al*. "SECRET—Secure Network Coding for Reduced Energy next Generation Mobile Small Cells: A European Training Network in Wireless Communications and Networking for 5G." *Internet Technologies and Applications (ITA)*, pp. 329–333. 2017.

[2] Q.U.A. Nadeem, *et al.*, "Design of 5G full dimension massive MIMO systems," *IEEE Trans. Commun.,* vol. *66*, pp. 726–740, 2018.

[3] A. Osseiran, *et al.,* "Scenarios for 5G mobile and wireless communications: the vision of the METIS project," *IEEE Commun. Mag.,* vol. 52, pp.26-35, 2014.

[4] Sharawi, M. S. *Printed MIMO antenna engineering*. 2014, Norwood, MA, USA: Artech House.

[5] N. O. Parchin, *et al.,* "Eight-element dual-polarized MIMO slot antenna system for 5G smartphone applications," *IEEE Access*, vol. 9, pp.15612-15622, 2019.

[6] N. O. Parchin *et al.,* "Multi-band MIMO antenna design with user-impact investigation for 4G and 5G mobile terminals, *Sensors*, vol. 19, pp. 1-16, 2019.

[7] N. O. Parchin, *et al.,* "Dual-polarized MIMO antenna array design using miniaturized self-complementary structures for 5G smartphone applications," *EuCAP Conference*, 31 March-5 April 2019, Krakow, Poland.

[8] M.-Y. Li, *et al*., "Tri-polarized 12-antenna MIMO array for future 5G smartphone applications," *IEEE Access,* vol. 6, pp. 6160–6170, 2018.

[9] R. Hussain, *et al*., "4-element concentric pentagonal slot-line-based ultra-wide tuning frequency reconfigurable MIMO antenna system," *IEEE Trans. Antennas Propag.*, vol. 66, pp. 4282–4287, 2018.

[10] N. O. Parchin, *et al.*, "Design and performance investigation of an eight-port MIMO antenna for 2.6 GHz LTE mobile terminal," *PhotonIcs and Electromagnetics Research Symposium*, 17-20 December 2019, Xiamen, CHINA.

[11] M. Abdullah, *et al.*, "Eight-element antenna array at 3.5GHz for MIMO wireless application," *PIER C,* vol. 78, pp. 209-217, 2017.

[12] N. O. Parchin, *et al.*, "8×8 MIMO antenna system with coupled-fed elements for 5G handsets," *The IET Conference on Antennas and Propagation (APC)*, 11-12 November, 2019, Birmingham, UK.

[13] Y. Li, *et al.,* "High-isolation 3.5-GHz 8-antenna MIMO array using balanced open slot antenna element for 5G smartphones," *IEEE Trans. Antennas Propag.,* 2019, doi:10.1109/TAP.2019.2902751.

[14] A. Zhao, R. Zhouyou, "Size reduction of self-isolated MIMO antenna system for 5G mobile phone applications," *IEEE Antennas and Wireless Propagation Letters*, vol. 18, pp. 152-156, 2019.

[15] N. O. Parchin, *et al.*, "Mutual coupling reduction of a closely spaced dual-band MIMO patch antenna array for 4G/5G applications," *PhotonIcs and Electromagnetics Research Symposium*, 17-20 December 2019, Xiamen, CHINA.

[16] P. Salonen, *et al.*, "A small planar inverted-F antenna for wearable applications", *IEEE International Symposium on Wearable Computers*, pp. 96- 100, 1999.

[17] N. Ojaroudi, *et al.*, "An omnidirectional PIFA for downlink and uplink satellite applications in C-band," *Microwave and Optical Technology Letters*, vol. 56, pp. 2684-2686, 2014.

[18] N. Ojaroudi, H. Ojaroudi, and N. Ghadimi, "Quad-Band Planar Inverted-F Antenna (PIFA) for Wireless Communication Systems," *Progress In Electromagnetics Research Letters*, vol. 45, pp. 51-56, 2014.

[19] Statement: Improving Consumer Access to Mobile Services at 3.6 GHz to 3.8 GHz. Available online: https://www.ofcom.org.uk/consultations-and-statements/category-1/future-use-at-3.6-3.8-ghz (accessed on 21 October 2018).

[20] *CST Microwave Studio*, ver. 2017, CST, Framingham, MA, USA, 2017.

[21] A. Musavand, *et al.,* "A compact UWB slot antenna with reconfigurable band-notched function for multimode applications," *Appl Comp Electromagn Soc J,* vol. 31, pp. 14-18, 2016.

[22] M. M. Abdollahi, *et al.,* "Octave-band monopole antenna with a horseshoe ground plane for wireless communications," *Appl Comp Electromagn Soc J*, vol. 30, pp. 773-778, 2015.

[23] B. H. Siahkal-Mahalle, *et al.,* "A new design of small square monopole antenna with enhanced bandwidth by using cross-shaped slot and conductor-backed plane," *Microwave Opt Technol Lett,* vol. 54, pp. 2656–2659, 2012.

[24] N. O. Parchin, *et al.*, "Dual-band monopole antenna for RFID applications," *Future Internet*, vol. 11, pp. 1-12, 2019.

[25] J. Zolghadr, *et al.*, "UWB slot antenna with band-notched property with time domain modeling based on genetic algorithm optimization," *Applied Computational Electromagnetics Society Journal*, vol. 31, pp. 926-932, 2016.

[26] M. S. Sharawi, Printed multi-band MIMO antenna systems and their performance metrics [wireless corner], *IEEE Antennas Propag. Mag.,* vol. 55, pp. 218–232, 2013.

[27] I. T.E. Elfergani, *et al.,* "*Antenna fundamentals for legacy mobile applications and beyond*," Springer Nature, pp. 1-659, Sept., 2017.

[28] N. Ojaroudiparchin, *et al.,* "A switchable 3D-coverage phased array antenna package for 5G mobile terminals," *IEEE Antenna and Wireless Propagation Letters*, vol. 15, pp. 1747–1750, 2016.